Research article

Calibration and planning techniques for mobile robots in industrial environments

Evangelos Papadopoulos and Michael Misailidis
NTUA, Athens, Greece

Abstract
Purpose – This paper aims to provide a simple and cheap calibration method to improve the odometry accuracy and to present an alternative method for the control of the path produced by an already existed path planning method.
Design/methodology/approach – Through the integration of systematic odometry errors the robot's odometry parameters are estimated and through the replacement of a caster with an omniwheel the unmodeled sources of odometry errors are removed. The control of the paths shape is achieved through the definition of intermediate points and robots velocity at these points.
Findings – The paper finds that the odometry calibration method improves significantly odometry accuracy. Caster and omniwheel performance depends on the paths characteristics and on their quality. The use of intermediate points offers a very good control on the paths' shape.
Research limitations/implications – The paper encourages the manufacturers of casters and omniwheels to improve their quality. The described path planning method inevitably halts the robot at certain points. Further research must be done to avoid this drawback.
Practical implications – Odometry calibration has become a simple procedure and can be easily implemented by robot manufacturers or researchers to improve odometry accuracy.
Originality/value – The odometry calibration method significantly reduces systematic odometry errors and makes odometry reliable apart from cheap. The influence of caster and omniwheel to odometry is examined along with the influence of better controlled path shape.

Keywords Calibration, Robotics, Motion

Paper type Research paper

1. Introduction

Most industrial robots have a fixed base that limits their capability. During the last decades, there has been an effort to use autonomous mobile robots in industry for various purposes. Their use requires tackling of two fundamental problems, i.e. localization (knowing a robot's position at any time), and path planning (finding a path that satisfies the kinematic constraints, avoids obstacles, and drives the robot to a desired position). A number of localization techniques exist including landmark identification, triangulation, tracking cameras, accelerometer signal integration and odometry. Odometry is one of the earliest methods used and is still in heavy use due to the low cost and availability of the required sensors, its accuracy for short distances and its compatibility with other localization methods. The method is based on the measurement of the distance traveled by each mobile robot's wheel and uses rotational encoders mounted on wheel shafts. Usually, localization is fused with other complementary techniques for optimized results. Its wide use makes its improvement of paramount importance.

The current issue and full text archive of this journal is available at
www.emeraldinsight.com/0143-991X.htm

Industrial Robot: An International Journal
35/6 (2008) 564–572

[DOI 10.1108/01439910810909574]

Current odometry-based calibration methods include the UMBmark (Borensein and Freg, 1995, 1996), the method by Larsen *et al.* (1998) and the PC-method (Doh *et al.*, 2003). The UMBmark method applies to differential driven robots only. According to this method, the robot travels a square path of 4×4 m both clockwise and counterclockwise and from the final robot position, the ratio of its wheel radii and its wheel base (the distance between the wheel centers) are calculated. According to the second method, an augmented Kalman filter is employed in order to estimate a correction to the nominal values of the wheel radii and its wheelbase. Finally, the PC-method proposes that the mobile robot moves along a path and localization odometry is employed in parallel to another very accurate localization method. The odometry parameters are calculated so that the difference between the estimated position with odometry and the other method is the least.

As far as the path planning with obstacle avoidance problem is concerned, various methods have been proposed. Jacobs and Canny (1989) have proposed the design of paths as a combination of arcs and straight lines. A method that keeps a robot at the maximum distance from obstacles and considers the nonholonomic constraint of mobile robots has been proposed (Mirtich and Canny, 1992). A method that takes into account kinematic constraints and the dynamics of the robot and achieves velocities up to 1 m/s has been developed (Schlegel, 1998). Smooth trajectories that can be used for obstacle avoidance were constructed by Quinlan and Khatib (1993). A method that considers robot velocity and allows its

Industrial Robot: An International Journal
Volume 35 · Number 6 · 2008 · 564–572

motion at high speeds has been developed (Fox *et al.*, 1997). Finally, a method has been developed that is based on the combination of dynamic window, elastic band and NF1 (Philippsen and Siegwart, 2003). This method results in smooth motions efficiently, both computationally and in the sense of goal-directedness.

In this paper, methods that improve the odometry-based localization ability of mobile robots in industrial environments are presented. A new robot calibration method is developed, that yields estimates of the main odometry parameters, responsible for systematic errors. According to this method, integrated odometry errors are compared to actual path errors to iteratively yield estimates of the main odometry parameters. Furthermore, we study and explain the caster's influence on odometry accuracy and evaluate experimentally its replacement with an omnidirectional wheel (omniwheel). The path planning method in Papadopoulos and Poulakakis (2000) and Papadopoulos *et al.* (2002) that takes into account the nonholonomic constraint and workspace obstacles, and produces a computationally inexpensive smooth path is presented briefly. In this method, the path is determined using the initial and final points of the path. The method is amended here to allow for the definition of intermediate points with prescribed velocities. This makes the resulting path shorter and eliminates unwanted path cusps, improving the odometry properties of the robot.

2. Odometry calibration method

The main disadvantage of odometry, is that it suffers from systematic as well as stochastic errors. Stochastic errors are caused by factors that cannot be predicted and affect a robot's odometry in an unpredictable way. In an industrial environment, they are usually less important than systematic errors, whose influence remains constant and accumulates throughout the path. There are many sources of systematic odometry errors such as differences between the nominal and the actual values of odometry parameters, variations of the wheel diameters due to centrifugal forces or variations of temperature, slippage of the wheels due to fast acceleration or sudden stop or skidding, etc. A large number of factors that affect odometry accuracy are described in Borensein and Freg (1996). Even if modeling of most of these factors were possible, practice has shown that the number of unknown parameters increases greatly, and the resulting model becomes too complicated to be useful in the correction of errors. On the other hand, the influence of a small number of odometry parameters (main odometry parameters) on odometry errors is much more serious in mobile robots in industrial environments. In addition, modeling the effects of the main parameters results in odometry models that can be handled relatively easily. This is the reason for which most of the efforts focusing on the improvement of the odometry accuracy, aim at estimating the main odometry parameters only.

In this section, we present a method that allows the precise estimation of the main odometry parameters for a mobile robot moving in an industrial environment. The method finds an expression that connects the final odometry error with the errors in odometry parameters through the integration of the odometry errors along the robot path. The expression is solved with respect to the odometry parameters and an iterative procedure is employed to improve the estimates. Here, we apply this calibration method on a differential drive robot. This drive type is the most common in mobile robots and consists of two independently driven wheels with tires and a caster wheel for stability.

The odometry of a differential drive robot (Figure 1) is based on the integration of the following kinematic equations:

$$\dot{x} = V_S \cos\theta \quad \dot{y} = V_S \sin\theta \quad \dot{\theta} = \omega \tag{1}$$

where θ is the robot's orientation, ω is its rotational speed, $\dot{x}$ and $\dot{y}$ are the x, and y components of its translational speed V_S.

The V_S and ω are given by:

$$V_S = \frac{\omega_r R_r + \omega_l R_l}{2} \quad \omega = \frac{\omega_r R_r - \omega_l R_l}{D} \tag{2}$$

where ω_r and ω_l are the angular speeds of the right and left driven wheels, respectively, R_r and R_l are their radii, and D is the distance between the centers of the driven wheels (Figure 1). Speeds ω_r and ω_l are found using the wheel encoders. Finding estimates of R_r and R_l and D, assumed to be unknown but constant, is the focus of the proposed method.

The main problem of odometry is that even small errors in the main odometry parameters R_r and R_l and D result in large and growing errors in the estimated robot position due to the integration of equation (1). The errors in these parameters are defined by:

$$\delta R_r = \hat{R}_r - R_r \quad \delta R_l = \hat{R}_l - R_l \quad \delta D = \hat{D} - D \tag{3}$$

where the $\hat{}$ indicates an estimate. These errors are systematic and not stochastic. Another systematic error, is due to the uncertainty in the parallelism of the robot fixed coordinate system and its estimated coordinate system (Figure 2):

$$\delta\phi_0 = \hat{\phi}_0 - \phi_0. \tag{4}$$

The nominal estimate $\hat{\phi}_0$ is taken equal to zero. We define as $\mathbf{P}$ the parameter error vector:

$$\mathbf{P} = [\delta R_r, \delta R_l, \delta D, \delta\phi]^T. \tag{5}$$

In the presence of a misalignment, the estimated robot linear and rotational speeds are given by:

Figure 1 Differences between nominal and actual parameter values

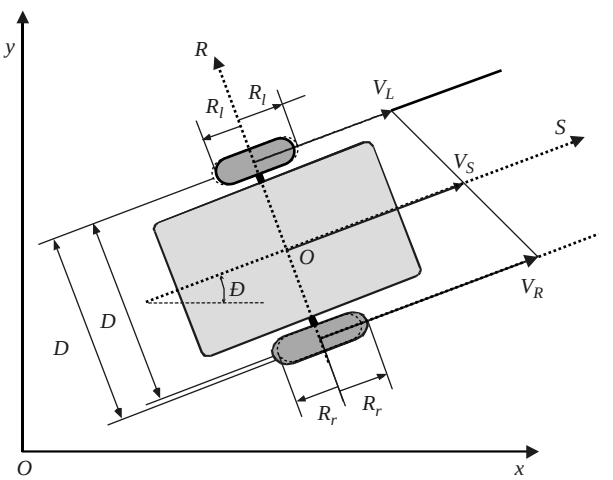

Figure 2 Robot initial orientation misalignment φ_0 results in position errors

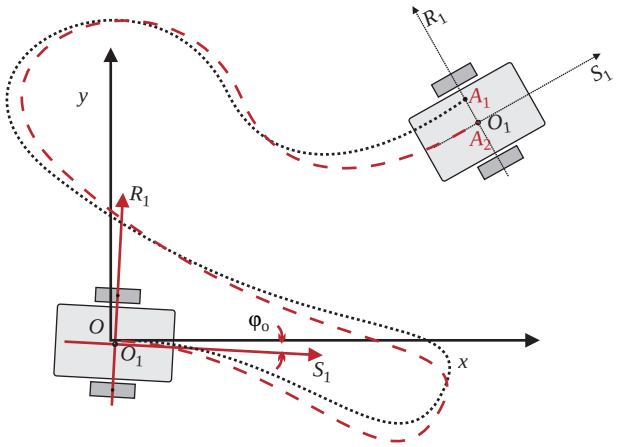

$$\hat{x} = \hat{V}_S \cos(\hat{\theta} + \hat{\phi}_0) \quad \hat{y} = \hat{V}_S \sin(\hat{\theta} + \hat{\phi}_0) \quad \hat{\dot{\theta}} = \hat{\omega} \tag{6}$$

$$\hat{V}_S = \frac{\omega_r \hat{R}_r + \omega_l \hat{R}_l}{2} \quad \hat{\omega} = \frac{\omega_r \hat{R}_r - \omega_l \hat{R}_l}{\hat{D}} \tag{7}$$

where, $\hat{x}, \hat{y}$ and $\hat{\dot{\theta}}$ are the estimated robot speeds, in contrast to $\dot{x}, \dot{y}$ and $\dot{\theta}$ which are the true ones, and can be found from Equations (6) and (7). Integrating Equation (6) along a path S, yields estimates of the robot's final position and orientation:

$$\hat{x} = \int_S \hat{V}_S \cos(\hat{\theta} + \hat{\phi}_0) \mathrm{d}t \quad \hat{y} = \int_S \hat{V}_S \sin(\hat{\theta} + \hat{\phi}_0) \mathrm{d}t \quad \hat{\theta} = \int_S \hat{\omega} \mathrm{d}t \tag{8}$$

Using equations (3), (4), (6) and (7), the speed errors due to parameter errors are written as:

$$[\delta\dot{x}\ \delta\dot{y}\ \delta\dot{\theta}]^{\mathrm{T}} = [\hat{\dot{x}} - \dot{x}, \hat{\dot{y}} - \dot{y}, \hat{\dot{\theta}} - \dot{\theta}]^{\mathrm{T}} = \mathbf{J} \cdot \mathbf{P} \tag{9}$$

where:

$$\mathbf{J} = \begin{bmatrix} \frac{\omega_r}{2}\cos(\hat{\theta} + \hat{\phi}_0) - V_S \frac{\theta_r}{\hat{D}} \sin(\hat{\theta} + \hat{\phi}_0) & \frac{\omega_r}{2}\cos(\hat{\theta} + \hat{\phi}_0) + \hat{V}_S \frac{\theta_l}{\hat{D}} \sin(\hat{\theta} + \hat{\phi}_0) \\ \frac{\omega_r}{2}\sin(\hat{\theta} + \hat{\phi}_0) + \hat{V}_S \frac{\theta_r}{\hat{D}} \cos(\hat{\theta} + \hat{\phi}_0) & \frac{\omega_l}{2}\sin(\hat{\theta} + \hat{\phi}_0) - \hat{V}_S \frac{\theta_l}{\hat{D}} \cos(\hat{\theta} + \hat{\phi}_0) \\ \frac{\omega_r}{\hat{D}} & -\frac{\omega_l}{\hat{D}} \end{bmatrix}$$

$$\begin{bmatrix} \hat{V}_S \frac{\hat{\theta}}{\hat{D}} \sin(\hat{\theta} + \hat{\phi}_0) & \hat{V}_S \sin(\hat{\theta} + \hat{\phi}_0) \\ -\hat{V}_S \frac{\hat{\theta}}{\hat{D}} \cos(\hat{\theta} + \hat{\phi}_0) & -\hat{V}_S \cos(\hat{\theta} + \hat{\phi}_0) \\ \frac{\omega_r}{\hat{D}} & -\frac{\omega_l}{\hat{D}} \end{bmatrix}. \tag{10}$$

Defining as X the error between the nominal $(\hat{\ })$ and actual position and orientation at the end of a path:

$$X = \begin{bmatrix} \delta x \\ \delta y \\ \delta\theta \end{bmatrix} = \begin{bmatrix} \hat{x} - x \\ \hat{y} - y \\ \hat{\theta} - \theta \end{bmatrix} \tag{11}$$

and since the main odometry parameters are constant, arithmetic integration along S yields:

$$X = \left(\int_S \mathbf{J} \cdot \mathrm{d}t \right) \cdot \mathbf{P} = \mathbf{K} \cdot \mathbf{P} \tag{12}$$

Equation (12) describes the fact that small variations in the wheel radii, the distance between the wheel centers, and the orientation inaccuracy result in errors to robot position and orientation. The new idea here is that since we have linearly connected the variations of odometry parameters in vector $\mathbf{P}$ with the errors at the final robot position and orientation, we can solve Equation (12) with respect to $\mathbf{P}$ and obtain new and more accurate values for the odometry parameters.

Matrix $\mathbf{K}$ can be found through arithmetic integration of equation (10) with time along the robot's path. To this end, the estimated, i.e. the nominal values $\hat{R}_r, \hat{R}_l, \hat{D}$ and $\hat{\phi}_0$, and the angular wheel speeds ω_r and ω_l are used. Vector $\mathbf{X}$ is found by subtracting the estimated robot position found by integrating Equation (6), from its measured (real) position, measured on the industrial floor.

Equation (10) is not enough for solving the problem, as the number of unknowns is four, while the equations are three. However, if the robot executes two paths, then enough equations exist to solve for the unknown vector $\mathbf{P}$ using least squares:

$$\begin{matrix} X_1 = K_1 \cdot \mathbf{P} \\ X_2 = K_2 \cdot \mathbf{P} \end{matrix} \quad \text{or} \quad \begin{bmatrix} X_1 \\ X_2 \end{bmatrix} = \begin{bmatrix} K_1 \\ K_2 \end{bmatrix} \mathbf{P}. \tag{13}$$

In practice, due to measurement errors, and to ensure a full rank for the augmented $\mathbf{K}$ matrix, it is preferable to use an augmented set of equations that result from a set of five experiments:

$$\begin{bmatrix} X_1 \\ X_2 \\ X_3 \\ X_4 \\ X_5 \end{bmatrix} = \begin{bmatrix} K_1 \\ K_2 \\ K_3 \\ K_4 \\ K_5 \end{bmatrix} \mathbf{P} \quad \text{or} \quad \mathbf{X}_{\text{full}} = \mathbf{K}_{\text{full}} \cdot \mathbf{P}. \tag{14}$$

Vector $\mathbf{P}$ is then calculated using the pseudoinverse of as:

$$\mathbf{P} = \left[\left((\mathbf{K}_{\text{full}})^{\mathrm{T}} \cdot (\mathbf{K}_{\text{full}}) \right)^{-1} (\mathbf{K}_{\text{full}})^{\mathrm{T}} \right] \cdot \mathbf{X}_{\text{full}}. \tag{15}$$

The odometry parameters that result using Equations (5) and (15) are given by:

$$\begin{matrix} R_r = \hat{R}_r - \delta R_r \quad R_l = \hat{R}_l - \delta R_l \quad D = \hat{D} - \delta D \\ \phi_0 = \hat{\phi}_0 - \delta\phi_0. \end{matrix} \tag{16}$$

The above procedure yields a better estimate for the odometry parameters. However, $\mathbf{K}_{\text{full}}$ is a function of $\hat{R}_r, \hat{R}_l, \hat{D}$, and $\hat{\phi}_0$. Therefore, the estimation of the odometry parameters can be improved if an iterative procedure is used, in which the initial parameter estimates are replaced by the computed ones, till a convergence of the estimates is achieved. This iterative procedure is depicted in Figure 3. As shown there, the newly obtained values from Equation (16) are

Figure 3 Recursive calculation of odometry parameters

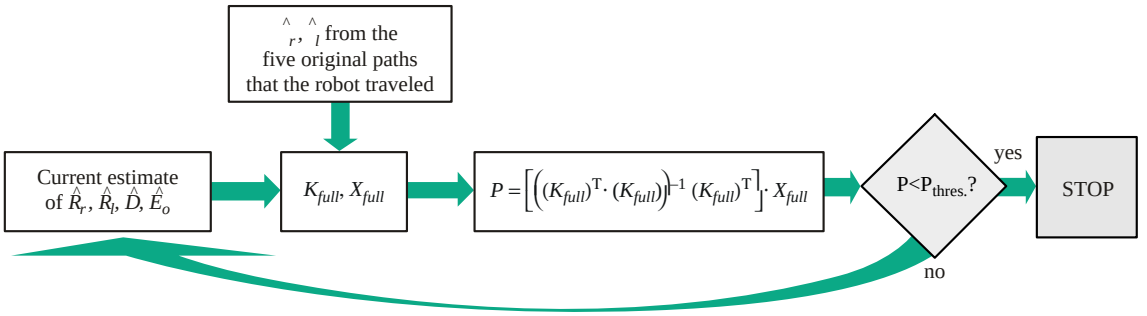

replaced into equation (10), a new $\mathbf{K}_{full}$ is computed, and a better estimate of the odometry parameters results. This repetitive procedure continues till the parameter error vector $\mathbf{P}$ falls below a prescribed threshold vector $\mathbf{P}_{thres}$.

The method proposed above has advantages when compared to the methods discussed in the Introduction, which have been proposed for the correction of systematic odometry errors. While the UMBmark assumes the average values of wheel radii known and yields only the ratio of R_r and R_l only, the proposed method calculates these radii independently. However, errors in the average values of robot wheel radii result in errors in the total length traveled by the robot. Furthermore, while UMBmark requires that the robot travels a 4 m × 4 m square path (several times if we want to reduce the influence of stochastic errors), in our method, the employed paths can be of arbitrary shape and length. This is a distinct advantage, as the paths can be chosen to be similar to the ones that the robot will travel while on duty, resulting in odometry parameters that will minimize the systematic odometry errors more appropriately. Moreover, UMBmark can be implemented to differential drive robots only, while our method can be implemented to any type of mobile robot as long as the appropriate differential kinematics equations are used. All we have to do is to express its velocities $\dot{x}, \dot{y}$ and $\dot{\theta}$ as a function of the main odometry parameters of the robot and of the known inputs, i.e. its motors angular velocities.

When compared to the method using the augmented Kalman filter, our method has the advantage of not requiring the use of expensive equipment such as a surveillance camera. In our method, we do not employ sensors other than the wheel encoders. Also, the identified odometry parameter values are in general close to the nominal ones. This is not always the case with other methods, such as the augmented Kalman filter method.

Finally, when compared to the PC-method, the proposed method has the advantage that it does not require the use of expensive equipment necessary in the PC-method for knowing the position and speed of the robot at all times. In our method, the only required measurement is measuring the robot final position and orientation.

As far as the accuracy of the method is concerned, it is was found experimentally that the accuracy of the proposed method appears to be better than that of the UMBmark, and in certain cases, comparable to the accuracy achieved by the PC-method. Due to the lack of the necessary equipment, no comparison could be made with the second method.

3. Caster replacement with an omniwheel

Up to now, we have presented a method that yields accurate odometry parameters. Beyond these, other factors exist that affect odometry, but were not modeled. A number of research works on differential drive robots, focus to other sources of odometry errors connected to the two driving wheels, ignoring the contribution of the caster wheel to such errors. Our experimental work showed that the behavior of the caster wheel is an important factor, influencing odometry significantly. While an ideal caster should not influence odometry at all, in practice manufacturing imperfections affect the accuracy of odometry. The imperfection mostly affecting odometry is the inclination of its base axis with respect to the vertical axis Z (Figure 4).

Due to this inclination, the ground reaction F has components F_1 and F_2.F_1 is parallel to the caster base axis and does not affect odometry. However, F_2 is perpendicular to the caster base axis and tends to rotate the caster base. On the other hand, when the robot moves, the plane of the caster wheel must be parallel to the movement direction. What parallelizes caster wheel plane with the movement direction is a friction force T, which tends to rotate the caster in the direction opposite to that of force F_2. Force T is an external friction force that exists even during straight robot motion, has a variable magnitude and direction depending on the path radius of curvature, and influences the robot motion throughout the entire path.

Figure 4 Inclination of caster base axis causes friction force T

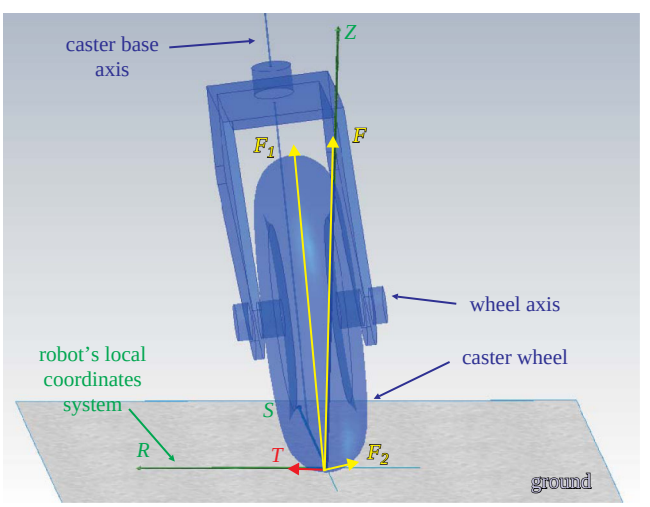

Industrial Robot: An International Journal
Volume 35 · Number 6 · 2008 · 564–572

Since modeling this disturbance is a complex task with uncertain practical gains, to minimize its effects we decided to replace the caster with an omniwheel (Figure 5). The wheel contains six barrels, arranged in two sides, that revolve and allow the movement of the wheel normal to its plane.

In theory, the only disturbance force that the omniwheel introduces is due to the shift of the point where the reaction of the ground is exerted as this reaction is exerted in alternation on one of the two wheel sides. In practice, more serious disturbance forces are introduced due to omniwheel defects. For example, for the wheel shown in Figure 5, the omniwheel was not absolutely circular, while a play existed along barrel longitudinal axes, causing sudden and rough movement of the robot. The later caused the main disturbance force, introduced by the omniwheel, and demonstrated in Figure 6.

As shown in Figure 6, the ground reaction F has components F_1 and F_2. Component F_1 is perpendicular to the axis barrel. Component F_2 is parallel to this axis and is counterbalanced by force R_2, exerted to the barrel from the right edge of the barrel's case (Figure 6(a)).

When the omniwheel rotates around its main axis and the inclination of the barrel's axis changes as in Figure 6(b), F_2 pushes the barrel on the left. Now force R_2 cannot be exerted until the barrel touches the left edge of the barrel's case. As a result, the omniwheel slides on the barrel's axis until the barrel collides to the left edge of the barrel's case. This sudden movement and collision introduces a disturbance force.

Comparing the caster and the omniwheel, one may notice that the disturbance forces introduced by the omniwheel appear instantly, when the inclination of the barrel's axis changes, and result in non-systematic odometry errors, while the disturbance force introduced by the caster affects odometry in a systematic way along the entire robot's path.

Figure 5 A typical omniwheel

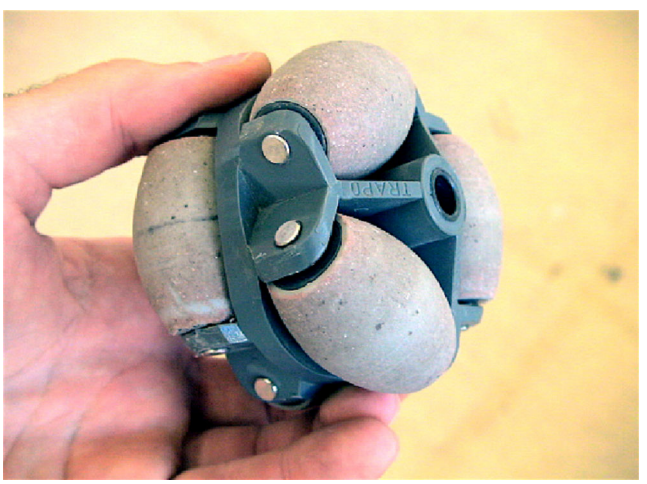

4. Experimental results

For the evaluation of the efficiency of the new calibration method and the influence of caster and omniwheel to odometry errors, a series of experiments using a Pioneer 3DX mobile robot (Figure 7) were conducted on a smooth indoor surface.

Four independent groups of experiments were conducted using the omniwheel or the caster, during which the robot traveled smooth paths or paths with abrupt turns including on-the-spot rotations. In each of these four groups of experiments, we followed the procedure described below. We placed the robot at the origin of the global coordinates system and five different paths of arbitrary shape and length between 5 and 50 m were used. The angular speeds ω_r and ω_l during the path and the final position and orientation were recorded. Using these and the nominal odometry values, $\mathbf{K}_{full}$ in Equation (14) and the estimated final position and orientation $\hat{x}, \hat{y}$ and $\hat{\theta}$ in Equation (8) were computed. Next, using these and the measured final positions and orientations, $\mathbf{X}_{full}$ in Equation (14) was calculated. Equation (15) yields $\mathbf{P}$ and with this, a new set of odometry parameters is found. The procedure is next repeated with the same recorded ω_r and ω_l and new odometry parameters to result in a new $\mathbf{K}_{full}$, and so on till the components of $\mathbf{P}$ are below 10^{-7}, indicating the calculation of the true odometry parameters.

To evaluate the accuracy of these parameters, the robot travels along and additional long path of at least 120 m. The evaluation is based on computing the following index:

$$d = \sqrt{(x_{real} - x_{est.})^2 + (y_{real} - y_{est.})^2} = \sqrt{(x - \hat{x})^2 + (y - \hat{y})^2} \quad (17)$$

Figure 6 Omniwheel forces. (a) The ground reaction component pushes the barrel to the right. (b) When the omniwheel rotates, F_2 changes direction and pushes the barrel to the left

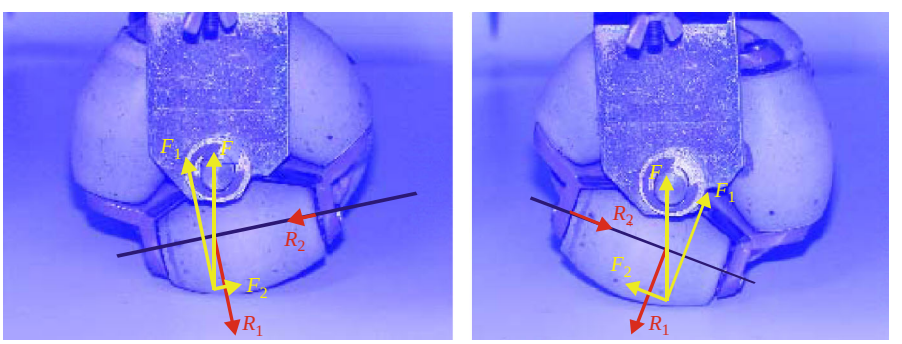

(a) (b)

Figure 7 Differential drive mobile robot

where the subscript real refers to the measured robot final position and est. to the estimated one (using the estimated true odometry parameters).

As mentioned above, we conducted four such groups of calibration experiments. In the first and third groups, the path radii of curvature was greater than 1 m. In the second and fourth groups, the path included parts of smaller radii of curvature and on-the-spot rotations. The results for index d are shown in Table I.

Looking at the second column of Table I, and comparing experiments 1 to 2 and 3 to 4, we conclude that small path radii of curvature result in an increase of odometry errors. Another conclusion, drawn by comparing experiments 1 to 3 and 3 to 4, is that the use of the omniwheel tends to reduce the odometry errors for the same path radii. The odometry errors before calibration method are attributed to systematic as well as to non-systematic errors.

Following the implementation of the calibration method, the influence of the systematic errors is regarded as limited, while non-systematic errors influence odometry accuracy to the same degree. Interpreting the experimental results in column 3 of Table I, we conclude that decreasing path radii increases odometry errors.

Comparing the odometry errors before and after the calibration for each experiment, we reach the following conclusions. In the first experiment, the calibration method reduces odometry errors approximately 8.5 times. However, in the second experiment, where the path's radius of curvature is less than 1 m, the odometry error remains significant. This is to be expected, since when the path's radius of curvature is small, the caster turns for a wider angle around its base axis, shown in Figure 4, and according to Section 3 and Figure 4, the variations of the force F_2 are bigger. Consequently, we conclude that when the path's radius of curvature is small, odometry errors caused by the caster are more prevalent. In the third and fourth experiments, the calibration method improves odometry accuracy about two times. The limited improvement is attributed to the increased influence of non-systematic errors introduced by the use of the particular omniwheel.

Table I Odometry experimental results

Experiment no.	Odometry error before calibration (cm)	Odometry error after calibration (cm)	Path length (m)	Notes
1	35.59	4.17	126.5	$r > 1$ m, caster
2	60.87	44.48	124.9	$r < 1$ m, caster
3	16.10	7.44	126.2	$r > 1$ m, omniwheel
4	37.03	14.14	124.8	$r < 1$ m, omniwheel

5. Path planning with intermediate points

In this section, we discuss a method that improves upon the path planning method for differential drive robots by Papadopoulos *et al.* (2002). This method, not only is fast in computing point-to-point trajectories, but it also provides obstacle avoidance. The improvements suggested here make the method more flexible by allowing the definition of intermediate points with prescribed speeds. The improved method yields smooth paths ensuring the continuity of the robot's velocity.

The original path planning method is reviewed here briefly. According to the method, the nonholonomic constraint of a differential drive robot, i.e.:

$$\sin\theta \mathrm{d}x - \cos\theta \mathrm{d}y = 0 \tag{18}$$

is transformed to:

$$\mathrm{d}u + v\mathrm{d}w = 0 \tag{19}$$

where u, v, w are expressed as functions of x, y and 0 through the invertible transformation:

$$\begin{aligned} u(x,y,\theta) &= x\sin\theta - y\cos\theta \\ v(x,y,\theta) &= x\cos\theta - y\sin\theta \\ w(x,y,\theta) &= \theta. \end{aligned} \tag{20}$$

Then, planning is done in the $u - v - w$ space, without the need to tackle the nonholonomic constraint, and the result is converted back to the $x - y - \theta$ space. The inverse transformation is:

$$\begin{aligned} x &= u(w)\sin w - v(w)\cos w \\ y &= -u(w)\cos w - v(w)\sin w \\ \theta &= w. \end{aligned} \tag{21}$$

Function w is selected to be a smooth function of time, while u and v are functions of w:

$$w = f(t) \tag{22}$$

$$u = g(w) \tag{23}$$

$$v = -\frac{\mathrm{d}u}{\mathrm{d}w} = -g'(w). \tag{24}$$

Notice that due to equation (24), the nonholonomic constraint is satisfied automatically.

The f and g functions can be taken to be any smooth functions. Here we choose polynomials. Their order is determined by the number of the boundary conditions they must satisfy, while their coefficients are determined by the boundary conditions.

The boundary conditions for $f(t)$ up to accelerations are:

$$\begin{aligned} f(t_0) &= w_0 = \theta_0 = \theta(t_0) \\ f'(t_0) &= \dot{w}_0 = \dot{\theta}_0 = \dot{\theta}(t_0) \\ f''(t_0) &= \ddot{w}_0 = \ddot{\theta}_0 = \ddot{\theta}(t_0) \\ f(t_f) &= w_f = \theta_f = \theta(t_f) \\ f'(t_f) &= \dot{w}_f = \dot{\theta}_f = \dot{\theta}(t_f) \\ f''(t_f) &= \ddot{w}_f = \ddot{\theta}_f = \ddot{\theta}(t_f). \end{aligned} \tag{25}$$

where the subscript 0 indicates the beginning and f the end of the path. To satisfy all of these, the order of $f(t)$ must be five, and have the form:

$$f(t) = a_5 t^5 + a_4 t^4 + a_3 t^3 + a_2 t^2 + a_1 t + a_0. \tag{26}$$

Using Equations (25) and (26), we obtain a linear system of six equations in six unknowns, a_i, $(i = 0, \ldots, 5)$, that can be solved.

The coefficients of $g(w)$ are determined by the robot initial and final position and translational speed. The coordinates of the initial and final position of the robot define the first four boundary conditions:

$$\begin{aligned} g(w_0) &= u_0 = x_0 \sin\theta_0 - y_0 \cos\theta_0 \\ g'(w_0) &= -v_0 = x_0 \cos\theta_0 - y_0 \sin\theta_0 \\ g(w_f) &= u_f = x_f \sin\theta_f - y_f \cos\theta_f \\ g'(w_f) &= -v_f = x_f \cos\theta_f - y_f \sin\theta_f. \end{aligned} \tag{27}$$

The original method is extended here to allow the definition of an intermediate point with desired speed V_S. To obtain a boundary condition for V_S, we use Equation (19) and differentiating Equation (20), we get:

$$\dot{x} = \cos w\dot{w}u - \cos w\dot{w} \quad \dot{y} = \sin w\dot{w}u - \sin w\dot{w}. \tag{28}$$

Using Equations (28) and (1), V_S is found to be:

$$V_S = u\dot{w} - v'\dot{w} \Leftrightarrow V_S = (g(w) + g''(w))\dot{w}. \tag{29}$$

Given a desired V_S at the initial or final time of a segment, Equation (29) provides an additional boundary condition for $g(w)$. The corresponding rate $\dot{w}$ is given in Equation (25).

Then, using all five conditions in Equations (27) and (29), a fourth order polynomial is obtained:

$$g(w) = b_4 w^4 + b_3 w^3 + b_2 w^2 + b_1 w + b_0. \tag{30}$$

Then, using Equations (27) and (29), we obtain a linear system of five equations with five unknowns, $b_i, (i = 0, \ldots, 4)$, that can be solved.

Having found f and g, u, v and w are found using Equations (22)-(24), and with the use of Equation (21) the coordinates and the orientation of the robot as a function of time are obtained.

The above analysis allows one to break a desirable path in segments and take boundary conditions for each segment. The advantage of this method is that it allows one to define intermediate points at which the robot's velocity can be the desired while with the original method was obligatory to stop the robot at each intermediate point. Obviously, it is important to ensure that the initial values for a path segment are equal to the final values for the previous one. As a result this method allows the creation of a more controllable path than the original one and the addition of as many intermediate points as we want without the problem of stopping the robot at the intermediate points. In addition, the occurrence of unwanted path cusps can be drastically reduced.

We may note here that the avoidance of cusps and starts and stops along the path results in shorter and smoother paths. In addition, stopping and starting over the robot repeatedly involves undue accelerations and decelerations, resulting in the deterioration of odometry accuracy. Continuity of the robot's speed along different path segments without having the robot stop at intermediate points has the advantage of a smoother motion and a reduction in odometry errors.

Note that whenever the rotational speed $\dot{\theta}$ is zero, also $\dot{\theta} = \dot{w} = 0$, and due to Equation (29), $V_S = 0$. Such cases may exist if one chooses an approximate path in which the orientation increases and then decreases (or the opposite), i.e. it has a turning point. Due to Equation (21), the robot will travel the same portion of the path forth and backwards. To avoid this, the approximate path must be broken in segments, in each of which the orientation θ is monotonous. For each of these segments, a different $g(w)$ is assigned. Therefore, if a path with a turning point is desired, this point must be defined as an intermediate one, with zero speed. The method is illustrated next with an example.

6. Simulation results

A quite difficult situation for the original method is the avoidance of an obstacle as in Figure 8.

Here the robot task is to begin from point (0,0) and reach the point at (10,10). The robot's orientation is the same at the beginning and the end of the path.

To solve this problem, we design an approximate desired path (Figure 9). Since this has two turning points, we choose

Figure 8 Initial and final robot configuration and obstacle

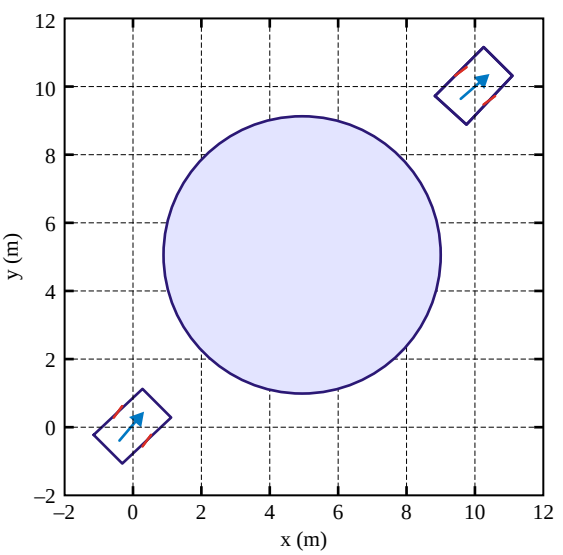

Figure 9 The desired path of the robot and intermediate points

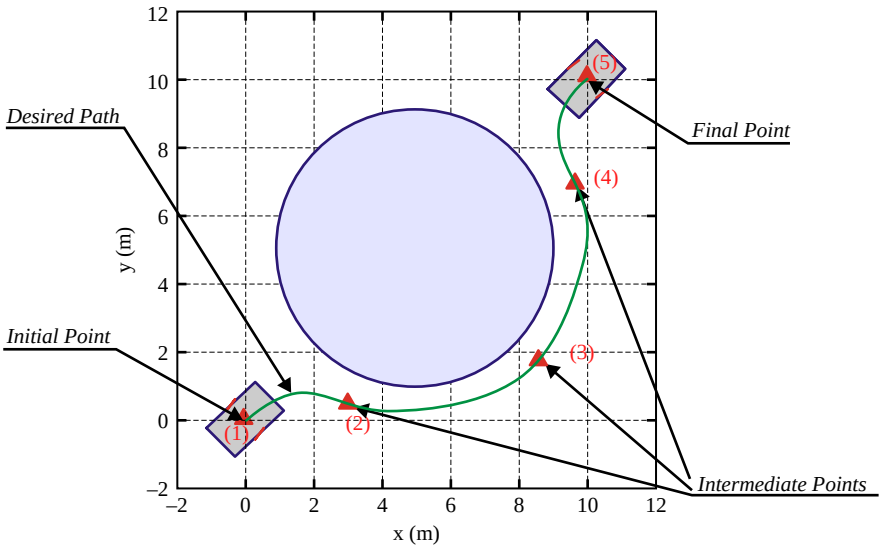

them as intermediate points (2) and (4), with zero speed (Figure 9). To ensure that the robot will not collide with the obstacle, a third intermediate point (3) with a prescribed speed is selected. Then, the total path is divided into four segments.

At point (1), the robot starts moving, so its rotational speed and acceleration is set to zero. Moreover, since its rotational speed is zero, its translational speed is also zero. Point (2) is a turning point and the robot rotational and translational speeds are zero. The rotational acceleration is positive, and to avoid the obstacle, the orientation is set to $\theta = -20°$. Since point (3) is not a turning point, its speeds are defined as desired. Point (4) is a turning point, like point (2). However, here the rotational acceleration must be negative. The boundary conditions for points (1)-(5) are shown in Table II. Using the above boundary conditions, the path planning method yields the path in Figure 10.

To obtain trajectories, it is important to set the time at which the robot will pass from intermediate points, and the final time. These parameters do not affect the shape of the path, but affect the required wheel speeds and the resulting robot speed. Decreasing the final time, the average speed of the robot along the path increases and vice versa. The translational velocity of the robot throughout the path is shown in Figure 11 for $t_{\text{final}} = 40$ s.

Table II Boundary and intermediate point conditions

	Point (1)	Point (2)	Point (3)	Point (4)	Point (5)
θ (°)	45	−20	45	100	45
$\dot{\theta}$ (°/s)	0	0	8	0	0
$\ddot{\theta}$ (°/s^2)	0	1	0	−3	0
x (m)	0	3	8.6	9.6	10
y (m)	0	0.5	1.8	7	10
V_S (m/s)	0	0	0.7	0	0

Figure 10 The resulting robot path

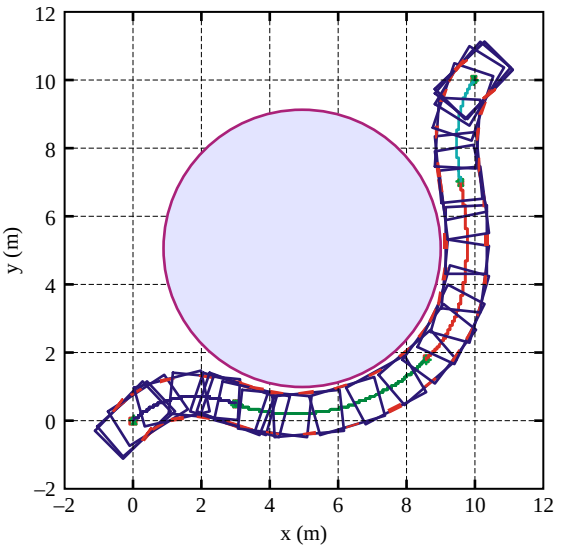

7. Conclusions

In this paper, techniques for mobile robots in industrial environments were developed. First, the localization accuracy of such robots employing odometry was considered. To address the localization problem, an odometry calibration method was used. The odometry errors were integrated along the entire path and new improved odometry parameters were calculated. An end-point method, with different initial and final points was used, while no sensors other than encoders were required. An important advantage of the proposed method is that it can fit any odometry model. The influence of the caster to odometry errors was also studied, and it was found that in general, the omniwheel yields improves the odometry accuracy. As far as the path planning problem is concerned, an existing method was extended, so that it can

Figure 11 The robot translational speed as a function of time

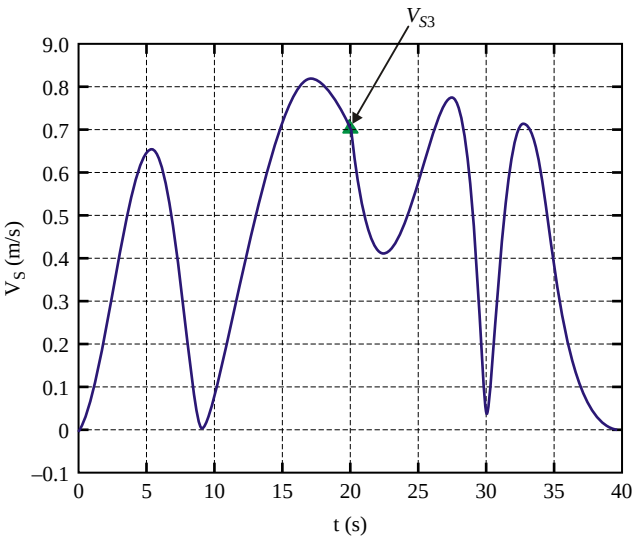

accept intermediate points with prescribed robot speeds. The result is a path shape that is more smooth and controllable, and improves odometry by reducing undesired acceleration and deceleration segments.

References

Borensein, J. and Freg, L. (1995), "Correction of systematic odometry errors in mobile robots", *Proceedings of the International Conference on Intelligent Robots and Systems, Pitchburgh, PA, August 5-9*, pp. 569-74.

Borensein, J. and Freg, L. (1996), "Measurement and correction of systematic odometry errors in mobile robots", *IEEE Trans. on Robotics and Automation*, Vol. 12 No. 6, pp. 869-80.

Doh, N., Choset, H. and Chung, W.K. (2003), "Accurate relative localization using odometry", *Proceedings International Conference on Robotics and Automation, Taipei, Taiwan, September 14-19*, pp. 1606-12.

Fox, D., Burgard, W. and Thrun, S. (1997), "The dynamic window approach to collision avoidance", *IEEE Robotics & Automation Magazine*, Vol. 4 No. 1, pp. 23-33.

Jacobs, P. and Canny, J. (1989), "Planning smooth paths for mobile robots", *Proceedings of the International Conference on Robotics and Automation, Scottsdale, AZ*, pp. 2-7.

Larsen, T.D., Bak, M., Andersen, N.A. and Ravn, O. (1998), "Location estimation for an autonomously guided vehicle using an augmented Kalman filter to autocalibrate odometry", *Proceedings of the FUSION98 SPIE Conference, Las Vegas, Nevada, USA, July.*

Mirtich, B. and Canny, J. (1992), "Using skeleton for nonholonomic motion planning among obstacles", *Proceedings of the IEEE International Conference on Robotics and Automation, Nice, France, May 1992*, pp. 2533-40.

Papadopoulos, E.G. and Poulakakis, I. (2000), "Planning and model-based control for mobile manipulators", *Proceedings of the International Conference on Intelligent Robots and Systems (IROS '00), Kagawa University, Takamatsu, Japan, October 30-November 5*, pp. 1810-5.

Papadopoulos, E.G., Poulakakis, I. and Papadimitriou, I. (2002), "On path planning and obstacle avoidance for nonholonomic platforms with manipulators: a polynomial approach", *The International Journal of Robotics Research*, Vol. 21 No. 4, pp. 367-83.

Philippsen, R. and Siegwart, R. (2003), "Smooth and efficient obstacle avoidance for a tour guide robot", *Proceedings of the International Conference on Robotics and Automation (ICRA 2003), Taipei, Taiwan, September 14-19*, pp. 446-51.

Quinlan, S. and Khatib, O. (1993), "Elastic bands: connecting path planning and control", *Proceedings of the IEEE International Conference on Robotics and Automation, Atlanta, GA*, pp. 802-7.

Schlegel, C. (1998), "Fast local obstacle avoidance under kinematic and dynamic constraints for a mobile robot", *Proceedings of the IEEE/RSJ International Conference on Intelligent Robots and Systems, Victoria, BC, Canada*, pp. 594-9.

Corresponding author

Evangelos Papadopoulos can be contacted at: egpapado@central.ntua.gr